POLISH MARITIME RESEARCH 4 (128) 2025 Vol. 32; pp. 20-32
10.2478/pomr-2025-0047

Hydrodynamic Assessment of Distributed Propulsion Systems for Shallow-Draft Inland Vessels

Martin Jurkovic [1, *]
Ladislav Illes [2]
Jarmila Sosedová [1]
Aditya Rio Prabowo [3]
Oleksiy Melnyk [4]
Ondrej Stopka [5]
[1] University of Žilina, Faculty of Operation and Economics of Transport and Communications, Žilina, Slovakia
[2] MULTI Engineering Services, Komarno, Slovakia
[3] Department of Mechanical Engineering, Faculty of Engineering, Universitas Sebelas Maret, Surakarta, Indonesia
[4] Department of Navigation and Maritime Safety, Odesa National Maritime University, Odesa, Ukraine
[5] Department of Transport and Logistics, Faculty of Technology, Institute of Technology and Business in Ceske Budejovice, Ceske Budejovice, Czechia

* Corresponding author: *martin.jurkovic@uniza.sk (Martin Jurkovic)*

ABSTRACT

This study investigates the hydrodynamic performance of three distributed propulsion configurations with distinct hull shapes. The influence of duct design and hull geometry on thrust, absorbed power, and the resulting thrust-to-power ratio is explored, and a computational fluid dynamics analysis is conducted with a focus on the relationship between the hull and propulsion system at a constant speed of 3 m/s. The results indicate that a pontoon-shaped hull with matching propulsion configuration yields optimal performance, with superior thrust-to-power ratios and hydrodynamic efficiency. In addition, a comprehensive design graph is presented, with the intention of aiding ship designers in selecting suiTable propulsion configurations for specific vessel types. The findings highlight the importance of integrating hydrodynamic and performance criteria into the design of distributed propulsion systems, and provide insights for the development of next-generation efficient inland vessels. Overall, the study provides practical guidelines for optimising distributed propulsion layouts in shallow-water vessel design.

Keywords: distributed propulsion system, propeller, restricted draft, CFD simulation

INTRODUCTION

Inland water transport represents an efficient means of cargo transportation, particularly for bulk cargo. It serves as a significant alternative to road and rail transportation, as it offers demonstrably lower transport costs per tonne-kilometre compared to these modes. The European Union is increasingly supporting inland water transport due to its ecological advantages and potential for technological innovation [1], but climate change has led to a deterioration in navigational conditions on Europe's inland waterways.

A main waterway in Europe is the Rhine-Main-Danube corridor, which connects the North Sea to the Black Sea. Persistent challenges, particularly associated with restricted navigation conditions on critical sections of the Danube, impose seasonal constraints and sometimes impede the operation of large vessels and convoys [2]. The smooth operation of inland navigation is primarily limited by variable water levels, especially during low- and high-water seasons. These constraints often result in restricted or halted navigation, meaning that vessels must be structurally adapted to cope with these limiting conditions in order to maximise navigability. One approach is to optimise the hull shape and propulsion system. The unique effects of shallow-water flow necessitate a distinct design approach for inland vessels compared to those intended for unrestricted navigation, and study of the inland ships of Bangladesh has shown that the adoption of a design approach with a focus on restricted waterways can improve the energy efficiency of a ship by up to 20% [3]. However, this kind of design approach may vary from one country to another, primarily due to changes in the geographical conditions. Traditional propulsion systems for inland vessels have a small propeller diameter (D) due to the limited under-keel clearance (UKC), requiring them to operate at high speeds, which is not very efficient [4]. Zentari et al. presented a systematic experimental and numerical investigation of resistance and propulsion tests for different pusher-barge configurations in deep and shallow waters, which provided insight into the effects of shallow water on resistance and propulsion for coupled ships [5]. This geometric limitation strongly influences propulsive efficiency and cavitation behaviour.

In parallel with technological efforts to optimise hull and propulsion systems, a growing body of research is focusing on the broader safety and operational risks associated with inland and maritime navigation. Melnyk et al. examined key security concerns in shipping, and emphasised the need for risk-informed vessel design and operation [6]. Building upon this study, recent work by Melnyk et al. proposed a structured method for evaluating the quality of risk assessment in shipboard operations through expert review, thereby supporting more robust and informed decision-making processes for vessel operation planning [7].

The optimisation of ship propulsion is commonly implemented through the use of the fluid dynamics capabilities within the ANSYS software, based on a computational fluid dynamics (CFD) methodology. This approach facilitates the acquisition of essential data, including pressure, velocity, and turbulence profiles, thus enabling the determination of the optimal propeller rotation speed [8]. The CFD process is frequently complemented by physical model tests conducted in an experimental setting, although tests in a simulated environment are prerequisites for the comprehensive development of project documentation. Wang et al. provided an improved CFD simulation strategy for underwater vehicles that could be used to model the interaction of the hull, propeller, and rudder [9]. Aram and Mucha also carried out CFD analyses of different propeller models for ship manoeuvring in calm water [10].

The shape, design, and optimal propulsion of vessels are all essential aspects of safe and efficient navigation on inland waterways. Numerous studies have explored the hydrodynamic design of ships' hulls and propellers with the aim of optimising their efficiency. Factors determining the economic efficiency of inland vessel operations were outlined by Hekkenberg, and studies by Lackenby, Raven, Schlichting, and Ferreiro have investigated the impact of limited draft on vessel speed [11-15]. Effective operation relies on favourable hydrodynamic conditions around the vessel hull and in the propulsion area, and the flow patterns around the hull in shallow waters are different from those in unrestricted depths. This was highlighted by Rotteveel [16], whose research focused on vessel flow in restricted depths and took into consideration backflow effects, vessel suction to the bottom, and changes in wave shape generated by the vessel's movement. Tuck explored the hydrodynamics of shallow waters [17], while Saha et al. presented a computational method of improving hull shape that took into account wave resistance in shallow waters [18]. Franceschi et al. solved the intricate problem of the hull–propeller–rudder interaction [19]. Through the use of CFD models, this investigation enabled the calculation of the coefficients needed for the prediction of manoeuvres with remarkable agreement with the semi-empirical model, which not only contributed to a more accurate interpretation of hull–propeller–rudder interactions but also provided a profound understanding of the underlying physical problems associated with these complex hydrodynamic phenomena. Various aspects related to navigation and ship performance were considered in studies by Melnyk et al. and Shumylo et al. with regard to a ship's motion control system; these authors discussed various methods of improving efficiency and safety and presented a comprehensive evaluation of the impact of hull geometry on the manoeuvrability and propulsion parameters of a ship [20, 21].

A review of the literature on hull shape optimisation for vessels navigating under restricted conditions reveals that research in this domain has predominantly focused on hull shape optimisation and traditional stern propulsion. The issue of distributed propulsion, a novel concept in shipbuilding, has not been sufficiently explored. A distributed propulsion system consists of laterally positioned propulsion units in various configurations. Methodological approaches to this research have summarised in several studies [22, 23]; for example, Illes et al. evaluated five laterally arranged distributed propulsion layouts through CFD simulations in a pilot stage. These cases were studied under restricted draft conditions in shallow water with a minimum UKC of 0.3 m and unrestricted draft in deep water. The results indicated that distributed propulsion with six or eight units produced significantly higher thrust effects in shallow water than the traditional layout. The study also examined suiTable propellers, such as a propeller-duct, which proved most suiTable for distributed propulsion systems. Seven designs were tested, using various numerical flow analyses (CFD), and at the end of the selection process, two versions remained with oval-shaped ducts, which were robust and resistant to ventilation [24]. The results of the second stage of research are summarised in further research by Illes et al. [25].

This paper focuses on the interaction between the propulsors of a distributed propulsion system and the hull of a vessel with various configurations. The aim of this study is to solve the problems of the performance characteristics and the anticipated operational properties of the propulsors by finding the most suiTable bow-stern shape for optimal collaboration, with a propulsion system that is laterally and serially arranged. Of the three combinations of hull termination shapes investigated here, the vessel with a pontoon-shaped bow and stern achieves the best results. Although this paper does not present detailed pressure contour plots, the underlying CFD simulations are based on the solution of the Navier–Stokes equations, which inherently provide pressure and velocity fields at the ship's hull and in the wake of the propulsor. The pressure distribution and flow behaviour are qualitatively assessed at the CFD post-processing stage to guide hull and propulsor design decisions. While this study is limited to numerical simulations, the methodology applied here builds upon previously validated CFD approaches and duct geometries. The intention is to explore relative performance trends among different propulsion configurations under restricted waterway conditions.

Two new duct designs—types 7 and 8—were developed to improve propulsion efficiency in shallow water and to minimise ventilation near the free surface. The design of these ducts integrates advantages of previous LIVT variants, with the aim of improving pressure recovery and stability under varying operating conditions. The following section presents the CFD methodology applied to assess these newly developed duct types and their interaction with the hull.

METHODS

CFD was employed as the primary tool for simulating the hydrodynamic behaviour of the vessel and propulsion systems. The core principle of CFD involves creating a computational domain consisting of a geometric model in a discretised form (mesh), defining boundary conditions, and specifying physical properties, calculation methods, and possibly the external geometric boundaries of the flow area.

In CFD simulations related to sailing, the geometry of the model typically includes the outer surface of the hull, surrounded by a flow area, usually of hexahedral shape. This scenario represents external flow, where the fluid moves in the surrounding environment rather than within the computational geometry. Physical phenomena occur in a multiphase environment at the interface between water and air, significantly increasing the computational complexity.

All simulations were performed at full-scale Reynolds numbers corresponding to the vessel length and operating speed. For the representative case at $v = 3$ m/s, the Reynolds number based on hull length ($L = 100$ m) was approximately 3.0×10^8, ensuring turbulent flow conditions across the entire wetted surface. The parameters of the turbulence model and the near-wall resolution were selected accordingly.

A major limitation of CFD analysis is the number of mesh elements (and nodes). Each iteration of the calculation requires evaluation of the hydrodynamic state of individual elements, and an excessive number of elements can greatly increase the computational complexity and processing time, meaning that it is essential to minimise the number of elements without compromising the accuracy of the calculation. A high-quality mesh is characterised by elements with uniform size, geometric regularity, and a consistent distribution within the discretised area. A choice of an appropriate element size is essential to accurately capture the hydrodynamic properties of the flow, and velocities are a key factor when determining the dimensions of the model.

In all of the simulations conducted here, particular attention was paid to the near-wall resolution to ensure reliability of turbulence modelling. A layered prism mesh was used at the hull surface, with three inflation layers and a growth ratio of 1.2. The thickness of the first layer was chosen to ensure that the dimensionless wall distance (y^+) remained below 30 for most of the hull, to satisfy the requirements for the k–ω SST model. This approach strikes a balance between mesh density and computational cost, while maintaining sufficient resolution of the boundary layer for hydrodynamic prediction. The mesh quality was verified using the standard skewness and orthogonality criteria in ANSYS Fluent.

A three-level grid sensitivity study was initially performed at the setup stage of the CFD analysis to verify its numerical consistency and guide the selection of the final mesh density used in all comparative simulations. To ensure grid independence and numerical reliability, a verification protocol based on Richardson extrapolation and the grid convergence index (GCI) was implemented. Three hierarchical mesh levels (coarse, medium, fine) were used, with an approximately constant refinement ratio $r \approx 1.4$, representing a typical value applied in CFD grid convergence studies. The monitored quantities of interest were the total thrust of the propulsion system T and the hull resistance R at $v = 3.0$ m/s. The order of accuracy p was estimated from the standard Richardson equations, and the fine-grid GCI was defined using a safety factor $F_s = 1.25$.

At this stage of the research, only the fine and medium-mesh results were retained; the earlier coarse-mesh dataset is unavailable, so explicit GCI values are not reported. However, the verification procedure, monitored quantities, and convergence criteria (residuals, time averaging, and stability of integrated quantity of interest) are described so that this approach can be reproduced in future work.

The conclusions of this study are comparative, and are based on consistent CFD conditions (identical physics, boundary conditions, propeller RPM, and near-wall treatment). The k–ω SST turbulence model and near-wall resolution ($y^+ < 30$) followed proven CFD practices for hull–propeller interaction [19, 24, 25], to ensure that the results presented here are physically consistent. Although explicit GCI values could not be reported, due to the missing coarse grid data, a qualitative verification confirmed that the variation between the medium and fine grid results for the monitored quantities was less than 3%.

In terms of the motion state of the solid bodies at the boundaries of the computational domain, the individual regions of the mesh can be stationary, deformable, or dynamic (Fig. 1). In general, dynamic meshes can be used wherever the shape of the domain changes over time due to rotational or translational movement of its bounding surfaces. During the simulation, the dynamic mesh and the surrounding domain area must be continuously smoothed and refined, which places increased demands on computational power.

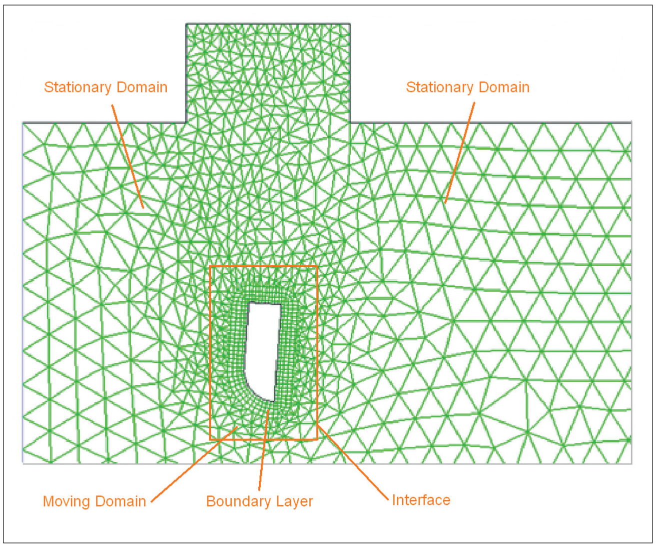

Fig. 1. Illustration of a dynamic mesh region in a 2D simulation (ANSYS Fluent 17.2 Documentation)

Several numerical methods have been developed to tackle specific physical problems, with the choice of method depending on both its suitability for the problem and its developmental history. By discretising the geometry of the studied area into a mesh of nodal points, the flow calculation domain is established, which allows the flow equations to be transformed into algebraic equations.

The finite volume method (FVM) is widely used in CFD simulations for solving the Navier–Stokes equations because it effectively maintains the principles of conservation for balanced physical quantities within the control volume. Research and development in the numerical modelling of turbulent flows continue to evolve, drawing on the latest advancements in mathematics, physics, and computational techniques; despite this progress, however, there is no universally applicable turbulence model that works effectively in all scenarios. Hence, the selection of the most appropriate model for a given calculation requires careful consideration of the strengths and limitations of each numerical model. The Reynolds-averaged Navier–Stokes (RANS) equations, in which time-averaged values of physical quantities are used to model turbulent flow, are increasingly popular in engineering simulations due to their relatively low computational requirements and accepTable accuracy. Various RANS methods have been developed for specific types of task, as they can simplify the modelling of swirls through additional transport equations [26].

The previous stages of the research have provided sufficient information for the development and further investigation of distributed arrangements of specific types of propulsors. In the first stage, the performance characteristics of the propulsion system were analysed [24]. The layout of the propulsors within the distributed propulsion system is shown in Fig. 2.

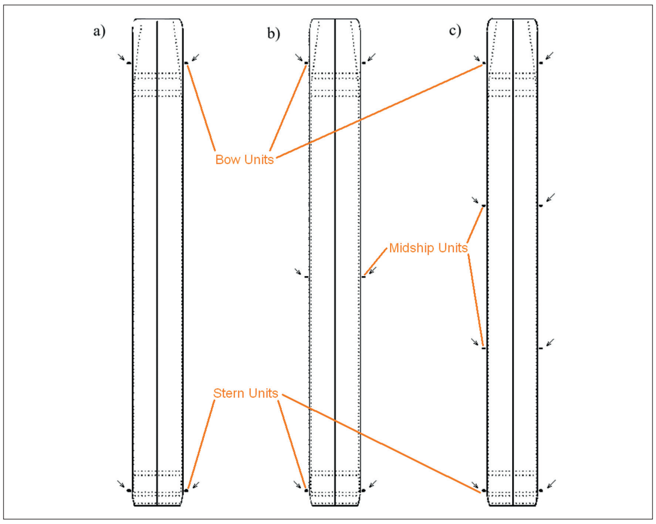

Fig. 2. Layouts of the distributed propulsion system (top view), showing various arrangements of side-mounted propulsors along the hull: (a) four side propulsion units mounted in the aft and fore hull zones (2 + 2, symmetrically); (b) six side propulsion units mounted in the aft, mid, and fore hull zones (2 + 2 + 2, symmetrically); (c) eight side propulsion units mounted evenly along the hull (2 + 2 + 2 + 2, symmetrically)

In the second stage of design, the focus was on how different configurations operate in conjunction with the vessel hull, and on comparing the thrust and performance values achieved. These results were also contrasted with the performance parameters and operation of traditional stern propulsion arrangements with the same hull [23]. The third stage sought to answer the question of whether it is advantageous to shape the bow and stern of the vessel specifically for optimal collaboration with distributed propulsion. In the analysis, three different stern-bow combinations were compared to guide the further development of ship hulls.

PERFORMANCE ANALYSIS OF PROPULSION UNITS IN A DISTRIBUTED PROPULSION SYSTEM

Four propulsors arranged in a row were placed in an open CFD channel with a hexagonal shape and limited depth (Fig. 3), in the presence of two phases: air and water. The interface between these phases formed a free surface in the channel. Based on our interpretation of results from previous studies, these analyses were conducted for units equipped with LIVT (an existing and proven geometry developed in St. Petersburg that serves as a basis for comparison with other cases) ducts of type 0, 3, 5, and 6, at a flow velocity of v = 3 m/s. Analyses were performed for propulsor spacings of 10D, 20D, 30D, and 40D, where D is the diameter of the propeller. The propeller diameter and rotational speed were uniformly set to D = 600 mm and n = 2000 RPM.

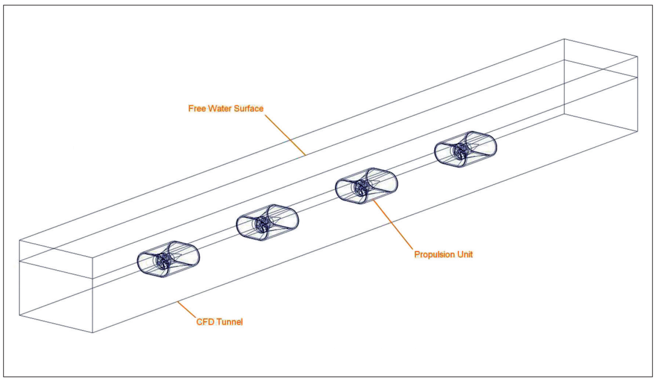

Fig. 3. 3D geometry of an open hexahedral CFD channel with four ducts

This geometry served as a simplified representation of the test environment for analysing the influence of the mutual spacing of the propulsion units. The regular geometry ensured repeatability of the simulations and minimisation of boundary condition errors. The basic dimensions are summarised in Table 1.

Tab. 1. Dimensions of hexahedral computational domains

Spacing	Length [m]	Width [m]	Height (limited) [m]	Water depth (limited) [m]
10D	27.5	3.0	2.5	1.8
20D	42.5	3.0	2.5	1.8
30D	57.5	3.0	2.5	1.8
40D	72.5	3.0	2.5	1.8

CFD analyses were conducted with the system parameters summarised in Table 2. Only the boundary conditions and initial values varied in each case.

Tab. 2. CFD system and calculation domain parameters

Software	ANSYS Fluent v. 17.2.0
Solver	Pressure, transient
Model	Liquid volume, multiphase, open tube
Euler's phases	Air, fresh water
Viscous model	Realisable k–ω SST model with low-Re wall treatment (suitable for resolving near-wall flows, with $y^+ < 30$ in prism layers)
Mesh type 1	Tetrahedral elements, propeller and duct area
Size of mesh elements 1	Min. 1 mm, max. 50 mm, controlled by curvature and proximity
Mesh type 2	Tetrahedral elements, filling the rest of the outer part of the CFD domain
Size of mesh elements 2	Min. 50 mm valid for the near zones, max. 200 mm valid for the far zones
Record	Drag force acting on the propulsor, propeller torque, mass flow through monitoring sections, total pressure in the monitoring areas

The aim of these analyses was to assess the performance characteristics of individual propulsor designs in collaboration, primarily focusing on thrust, shaft power, and the dependence on their mutual distance. The results are presented as comparative graphs to support further decision making.

Although all of the propulsors analysed in this study were of a ducted type, the effect of the duct on performance can be inferred from prior investigations and from the differences observed among the LIVT 0, 3, 5, and 6 configurations. Ducts significantly increase propeller thrust at low speeds by reducing tip vortex losses and improving flow direction, which is especially important for propellers with small diameters operating in shallow water. Previous studies suggest that non-ducted versions of comparable propellers may produce 20–30% less thrust under similar operating conditions. In future work, direct comparisons between ducted and non-ducted propellers may be performed using the same CFD methodology.

Analysis of hull–propulsion interaction

Two arrangements were analysed: a traditional configuration, in which propulsors were located beneath the stern of the vessel, and a serially distributed configuration with propulsors along the sides of the vessel. Models with both configurations, along with the hull model, were placed in an open CFD channel with a hexagonal shape and limited depth to simulate the presence of the air and water phases. The interface between these phases simulated a free surface in the channel. The same 3D hull model as used in the first stage was employed for these analyses.

This model illustrates the conventional aft-mounted propulsion arrangement, which serves here as a reference case. Fig. 4 provides insight into the geometrical constraints influencing the placement and size of propellers, which is relevant for a comparison with the distributed layouts. The traditional stern arrangement consisted of four (2+2) LIVT zero duct propulsors, with the maximum possible diameter for the stern, as depicted in Fig. 4. The diameter and rotation speed of the propellers were uniformly set to $D = 1150$ mm and $n = 450$ RPM. The analysis was conducted solely as a reference, at a navigation speed of $v = 3$ m/s.

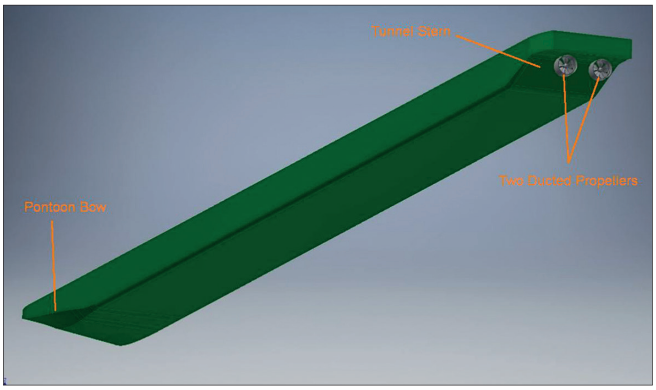

Fig. 4. Side view of hull with stern-mounted propulsion

Table 3 lists the main propeller parameters. All propeller dimensions are parametric and depend on the diameter, including the radius of curvature and the dimensions of the propeller cones.

Tab. 3. Main parameters of the propeller

Diameter [m]	Hub diameter [m]	Hub length [m]	Pitch [m]	Blade thickness [m]	Number of blades [pcs]	Area ratio [-]
D	D×0.24	D×0.24	D	D×0.02	5	0.805

The main dimensions of the computational domain are presented in Table 4. The computational domain was defined as a hexahedral open channel with a free surface, with a minimum clearance of three to five hull lengths before and after the ship model, in order to minimise backflow effects and artificial pressure reflections. The side clearance from the hull was set to at least twice the beam width, based on best practices for external flow simulations. Boundary conditions included the inlet/outlet pressure, planes of symmetry at the sides, and a moving reference frame that was applied around the propellers.

Tab. 4. Dimensions of the hexahedral computational domain

Length [m]	Width [m]	Height (limited) [m]	Water depth (limited) [m]
300	50.0	6.8	1.8

CFD analyses were conducted with the system parameters given in Table 5.

Tab. 5. Set CFD system and calculation domain parameters

Software	ANSYS Fluent v. 17.2.0
Solver	Pressure, transient
Model	Liquid volume, multiphase, open tube
Euler's phases	Air, fresh water
Viscous model	Realisable k–ω SST model with low-Re wall treatment (suitable for resolving near-wall flows, with $y^+ < 30$ in prism layers)
Mesh type 1	Tetrahedral elements, propeller and duct area
Size of mesh elements 1	Min. 5 mm, max. 100 mm, controlled by curvature and proximity
Mesh type 2	Tetrahedral elements, filling the rest of the outer part of the CFD domain
Size of mesh elements 2	Min. 50 mm valid for the near zones, max. 1000 mm valid for the far zones
Record	Drag force acting on the propulsor, propeller torque

Classic Kort nozzle and LIVT-type ducts yield excellent performance when well-enclosed, but these ducts are prone to ventilation (air entrainment) when close to the free water surface. This disadvantage manifested in some of the cases analysed here, resulting in reduced thrust and propulsive power loss, particularly under challenging wave conditions.

Based on our interpretation of previous studies, new types of propulsor were developed as part of our research on distributed arrangements, which are referred to here as types 7 (Fig. 5(a)) and 8 (Fig. 5(b)). These propulsors combined the favourable performance and hydrodynamic characteristics of ducts LIVT 0, 5, and 6. Propeller diameters and rotations were uniformly set to $D = 600$ mm and $n = 1500$ RPM, and the propulsor spacings were consistently set to 45D in an arrangement with eight propulsion units [24]. All analyses were conducted at navigation speeds of $v = 3.0$, 3.5, and 4.0 m/s. A 3D model of the propulsors is shown in Fig. 5.

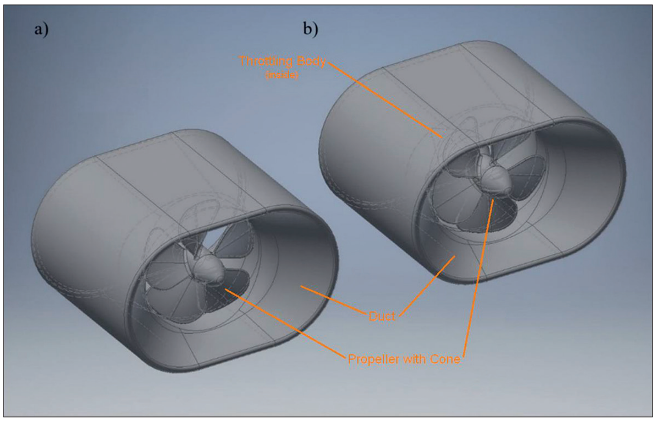

Fig. 5. 3D geometry of the propulsors (source: authors): (a) propulsor type 7; (b) propulsor type 8

Propulsor types 7 and 8 are almost identical, with the difference being that type 8 features an additional conical throttling body inserted into the internal space of the diffuser, serving as a seamless extension of the propeller charge. The cone enhances the efficiency of the propulsion unit by reducing the flow velocity and increasing the pressure on the outlet side, which proves advantageous at low speeds of advance and under high propeller loads. As the speed of advance (water flow) increases, the hydrodynamic characteristics of the duct become increasingly evident, and the resistance of the conical duct becomes more pronounced. The main dimensions of the propulsors are given in Table 6, and the 3D geometry of the hull with distributed propulsion is shown in Fig. 6.

Tab. 6. Main dimensions of the propulsor units

Length [mm]	Width [mm]	Height [m]	Radius (outer) [mm]
930	1105	720	360

Fig. 6 shows the longitudinal placement of the propulsion units along the hull sides, and indicates the intended interaction zones with surrounding flow fields and hull wake. CFD analyses were performed with the system parameters listed in Table 7. Only the boundary conditions and initialisation values differed between the cases.

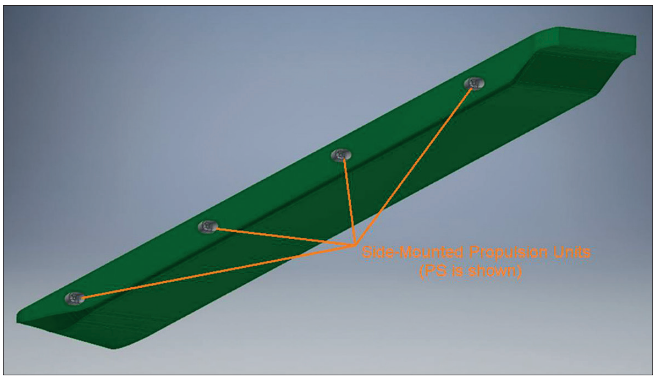

Fig. 6. 3D geometry of the hull with distributed propulsion system

Tab. 7. Parameters of the CFD system and calculation domain

Software	ANSYS Fluent v. 17.2.0
Solver	Pressure, transient
Model	Liquid volume, multiphase, open tube
Euler's phases	Air, fresh water
Viscous model	Realisable k–ω SST model with low-Re wall treatment (suitable for resolving near-wall flows, with $y^+ < 30$ in prism layers)
Mesh type 1	Prism elements, 3 layers above the hull surface, aspect ratio 10-7
Size of mesh elements 1	Min. 10 mm, max. 100 mm, controlled by curvature and proximity
Mesh type 2	Tetrahedral elements, propeller and duct area
Size of mesh elements 2	Min. 1 mm, max. 100 mm, controlled by curvature and proximity
Mesh type 3	Tetrahedral elements, filling the rest of the outer part of the CFD domain
Size of mesh elements 3	Min. 50 mm valid for the near zones, max. 1000 mm valid for the far zones
Record	Drag force acting on the propulsor, propeller torque, mass flow through monitoring sections, total pressure in the monitoring areas

The aim of these analyses was to determine the performance and hydrodynamic properties of individual propulsor designs in cooperation, particularly in terms of the thrust, shaft power, and dependence on mutual distance. The outcomes will be presented in the form of comparative values and graphs to support the evaluation process.

It should be noted that the simulations were carried out with fixed RPM settings, and do not represent fully coupled self-propulsion tests. Hence, the wake fraction and thrust deduction factors were not extracted separately, although their effects are inherently captured in the hydrodynamic interaction between the hull and propulsors in the simulation. The flow field includes pressure buildup, suction effects, and momentum recovery behind the ducts.

Analysis of the impact of bow and stern shapes

In the first stage of the investigation, a low-draft cargo ship hull was selected, with typical dimensions for the Danube–Main–Rhine (DMR) navigation area. Its bow and stern were shaped to make it suiTable for both traditional stern propulsion and potential alternative solutions. The design of the bow also allowed the vessel to be connected to a push convoy with a single barge. Three different variants with identical main dimensions were proposed for analysis, as described below.

(i) Variant PU (basic version from the first stage: P—pontoon bow, U—universal stern)

This PU hull type was also used in the first stage of the research, and is shown in Fig. 7.

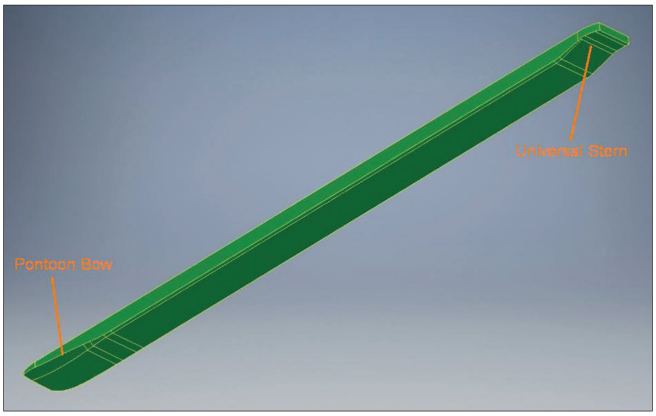

Fig. 7. 3D geometry of the PU hull

This configuration serves as a baseline for the performance comparison. The simplified overhanging stern generates flow detachment zones, which are reflected in reduced thrust-to-power ratios.

(ii) Variant PP (with only the bow from the original version: P—pontoon bow, P—pontoon stern)

To improve the flow patterns and mitigate stern waves, the stern shape was modified to a pontoon type, as this is better able to prevent sudden stream detachment and intense swirling compared to the original overhanging stern. The 3D design of the PP hull is shown in Fig. 8.

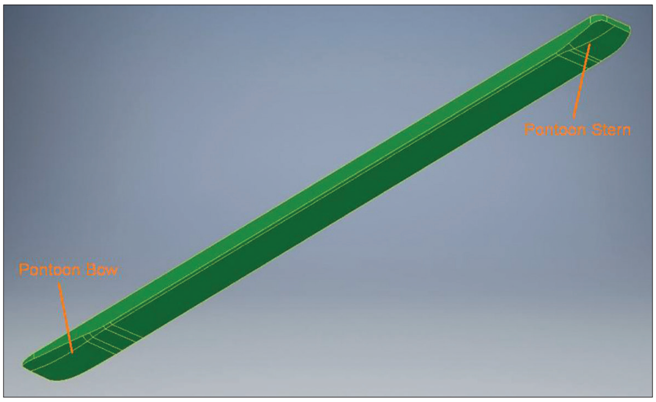

Fig. 8. 3D geometry of the PP hull

Fig. 8 shows the optimised pontoon shape, which is shown to mitigate vortex formation and allow for free shaping of the stern without propulsion shaft constraints.

(iii) Variant VP (stern derived from the PP version: V—V-shaped (U) bow, P—pontoon stern)

Although the V-shaped bow is disadvantageous for small H/B (height-to-beam) and T/B (draft-to-beam) ratios, it was considered due to its prevalent use in river cargo ships. A 3D model of the VP hull shape is shown in Fig. 9.

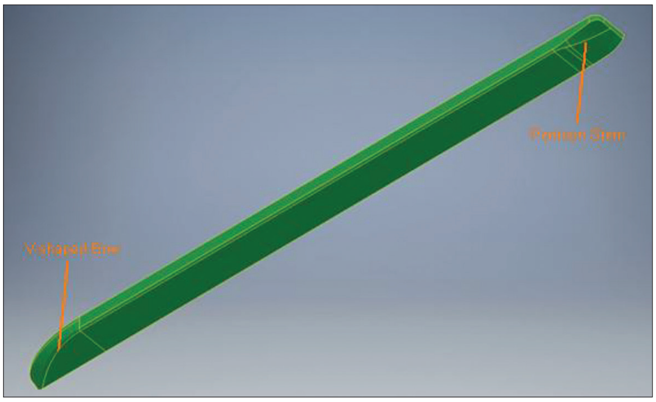

Fig. 9. 3D geometry of the VP hull

This geometry highlights the influence of conventional V-shaped bows, which are common in older vessels, and serves as a reference for understanding the limitations that wave-induced turbulence imposes on distributed propulsion.

All hull variants were based on a distributed propulsion arrangement with eight propulsors equipped with duct type 7. The diameter and rotation of each propeller were consistently set to $D = 600$ mm and $n = 1500$ RPM. All analyses were conducted at navigation speeds of $v = 3.0$, 3.5, and 4.0 m/s. The dimensions of the computational domain are listed in Table 4, while the parameters and settings of the CFD network are given in Table 6.

The objective of these analyses was to ascertain the diverse performance and hydrodynamic properties of three hull/propulsion configurations with the same distributed propulsion arrangement but varying shapes for the bow and stern. The outcomes are presented in the form of comparative values and graphs to aid in selecting the optimal variant.

RESULTS

In this study, the individual solutions from the second phase were no longer analysed in isolation standalone propulsors, regardless of the effects on the ship's hull. Based on the first-stage results, the investigation focused on the serial arrangement of the distributed propulsion system. - The geometry of the ducts was refined by creating two final versions (propulsors 7 and 8), and the optimal shapes for the hull, bow and stern were also investigated.

INTERACTION BETWEEN THE PROPULSORS AND THE DISTRIBUTED PROPULSION SYSTEM

Figs. 10 to 13 show comparative graphs of the results for a series of four propulsors in the arrangement shown in Fig. 2(c), equipped with LIVT 0, 3, 5, and 6 ducts. These figures demonstrate the dependency of the thrust and power of the distributed propulsion system on the mutual distance of the individual propulsors, assuming uniform spacing, identical geometry, and equal rotational speeds. The spacing is represented as a multiple of the propeller diameter, which is its characteristic dimension in similarity theory. The ship's side was considered in the computational CFD domain as a nearby vertical wall with viscous resistance to the flow. As expected, propulsors with LIVT 0 and 3 ducts experienced problems with ventilation, especially in position 4 (the most forward duct). The theoretical propulsors considered in the first stage also had similar problems in the bow area. Propulsors with duct 6 generated higher thrust than those with duct 5, at the cost of a higher absorbed power. These two versions differed only in the form of the exit cone, and had a relatively high resistance.

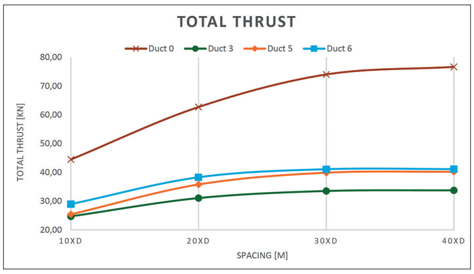

Fig. 10. Comparison of results for the total generated thrust of propulsors with varying spacing

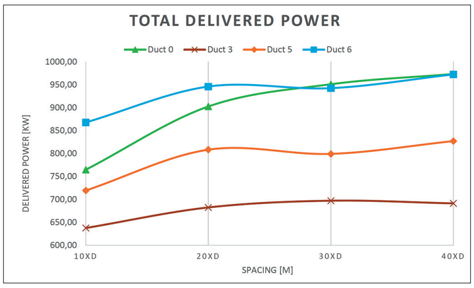

Fig. 11. Comparison of results for the total absorbed/delivered power with varying propulsor spacing

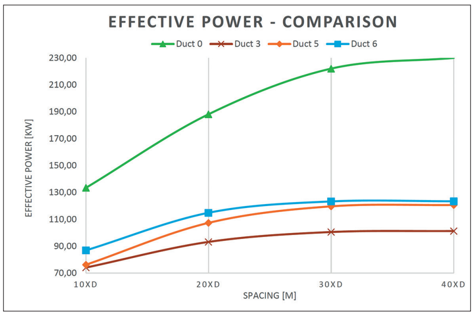

Fig. 12. Comparison of results for the total effective power with varying propulsor spacing

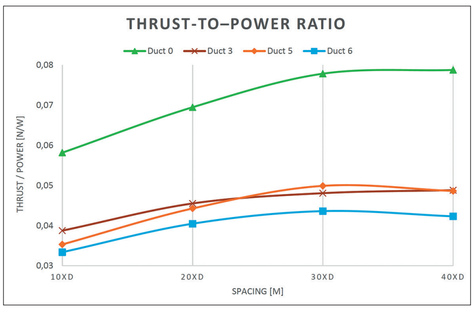

Fig. 13. Comparison of the Thrust-to-power ratio with varying propulsor spacing

In Fig. 11, the two parallel waves in the power curves indicate the presence of oscillations and 'resonant' states. Increasing the number of propulsors in the system also increases the number of uncertainties and the occurrence of oscillations. An appropriate analogy for this would be a pendulum: the motion of a double pendulum can be calculated, but for a triple pendulum, there is no satisfactory solution, and adding another element makes it unsolvable. In the present context, the more elements in the system, the higher the number of possible oscillations. These undesirable states pose serious challenges to numerical analyses; for instance, an unsteady state of the flow fields around the propulsors is likely to stabilise over time in reality, but this may not hold true for CFD simulations.

Figs. 10 to 13 exhibit very similar trends, with the performance reaching zero between spacings of 2D (physical boundary) and 10D. The curves asymptotically approach their maximum values, with their limiting value (for four propulsors) determined as four times the maximum of the observed quantity achieved under the same conditions for an individual propulsor. In particular, the higher thrust observed in the case of duct 0 (Fig. 10) results from the larger spacing used during the simulations, which significantly reduces the flow interference effects between the propulsion units. The maximum spacing in this case was 40D, which allowed for near-ideal inflow conditions. In contrast, other duct variants were evaluated at reduced spacing intervals to reflect more practical integration constraints. From a technical perspective, this distributed propulsion system achieves the maximum possible performance for a spacing of between 30D and 40D, where losses become negligible.

The losses associated with the spacing of serially arranged propulsors are caused by the mutual influence of their flow fields. When the propulsor spacing is small, the accelerated water flow on the outlet side of the front propulsor does not lose kinetic energy, which increases the flow velocity on the inlet side of the rear propulsor. This results in a decrease in the thrust force of the rear propulsor while increasing its efficiency. For the same reason, propulsors with high flow velocities on the outlet side must have larger spacings, and are generally not the most suiTable for this type of distributed propulsion system.

The detailed wake distributions and inflow velocities at the propulsor disc were not extracted in this study, although the mutual interaction effects between propulsors (especially at lower spacing values) were considered in the full 3D CFD analysis. The influence of wake and suction is therefore implicitly accounted for, but no explicit wake fraction or thrust deduction factor is presented.

INTERACTION BETWEEN THE HULL AND PROPULSION SYSTEM

Analyses of the interaction between the hull and propulsors were conducted on the modified ducts 7 and 8, whose proportions are much closer to real ducts with lower resistance. Their performance characteristics are presented in Figs. 14–17. The PU variant was used as the hull, similarly to the simulations in the first stage.

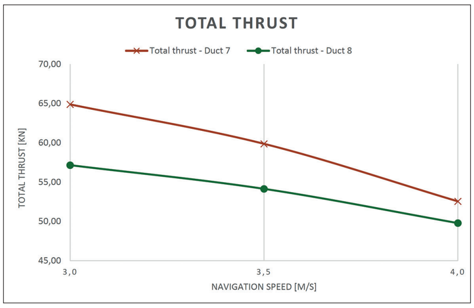

Fig. 14. Comparison of results for the total thrust generated by the propulsors

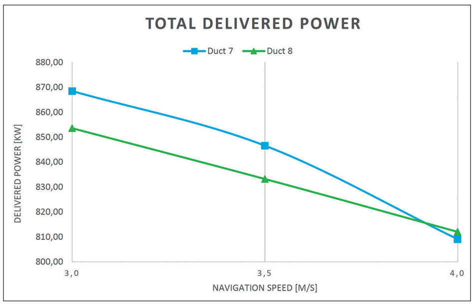

Fig. 15. Comparison of results for the total power absorbed/delivered by the propulsors

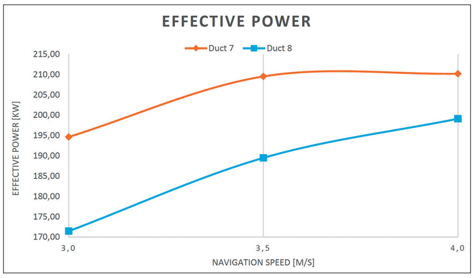

Fig. 16. Comparison of results for the total effective power of the propulsors

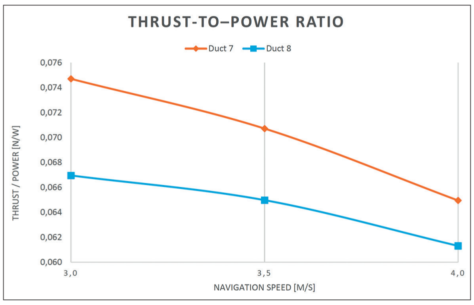

Fig. 17. Comparison of results for the Thrust-to-power ratio of the propulsors

The consistency of the numerical setup was verified through a mesh-convergence assessment that followed the GCI protocol described in the Methods section, to confirm the sTable thrust and resistance predictions across the tested grid levels and support the reliability of the comparative results presented here. To complement the quantitative results, additional attention was paid to a qualitative evaluation of the pressure distribution and free-surface behaviour around the hull. The pressure field analysis showed a moderate reduction in the pressure peaks in the aft region when the propulsors were active, indicating smoother flow recovery and reduced local separation. The free-surface contours contained only minor deformations in the stern zone, which are typical of shallow-water operation. These observations confirm that the CFD model realistically captured hydrodynamic features of the hull–propulsor interaction, without numerical instability. A visual representation of the pressure and free-surface contours will be included in future experimental validation work that will be undertaken to complement the numerical findings.

The equilibrium sailing speed of the vessel was determined numerically, based on the intersection of the total thrust and resistance curves. The resistance data were obtained from bare-hull simulations, whereas the thrust values were extracted from hull–propulsor configurations at various fixed propeller speeds. The intersection point represents the steady-state sailing condition, under which the thrust balances the total hydrodynamic resistance. For the cases analysed here, duct 8 achieved an equilibrium velocity of approximately 3.54 m/s, whereas the value for duct 7 was about 3.41 m/s, confirming the more efficient flow interaction of the arrangement of duct 8. This numerical intersection method was verified by interpolating between CFD data points and ensuring monotonic thrust and resistance behaviour across the investigated range.

Fig. 18 was produced by combining graphs of the generated thrust with the hull resistance curve. The intersection between the propulsor thrust and hull resistance curves represents the equilibrium point for the forces acting on the hull in the direction of motion. The resistance curve in Fig. 18 was derived from CFD simulations of the bare hull (without active propulsion), in which the resistance values were obtained by integrating pressure and viscous forces on the hull surface during steady forward motion. The analysis did not constitute a full self-propulsion test with control feedback; instead, fixed-RPM propulsion was used to study the system interaction. This defines the maximum achievable speed of the vessel with the given propulsion system. The curves in this type of graph are also referred to as 'desired' and 'achieved' thrust curves.

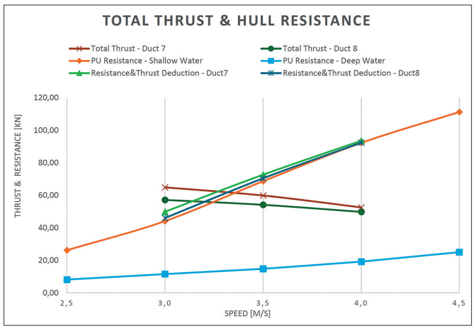

Fig. 18. Comparison of results for the total thrust of the propulsors and the resistance of hull (type PU)

Fig. 18 shows the resistance curve of the 'bare' hull (without propulsion) and two modified resistance curves, whose values were recorded during analyses of the interaction between the hull and propulsors 7 and 8. The intersections with these curves provide a more realistic value of the limiting speed, because they include the thrust increase caused by the propulsion system.

INFLUENCE OF THE SHAPE OF THE BOW AND STERN

To investigate the most suiTable shaping of the bow and stern of the ship's hull, versions PU, PP, and VP were considered for the distributed propulsion system, equipped with propulsion units fitted with duct 7 in a serial arrangement, as shown in Fig. 2(c). Due to the time-consuming nature of these computations, the joint operation analyses between the hull and propulsion were only performed for a speed of 3 m/s. The calculated values of the generated thrust, absorbed power, and the ratio between them are presented in Table 8.

Tab. 8. Performance parameters for the distributed propulsion system when operating with hulls of different shapes

Hull version	Stern (shape)	Bow (shape)	Generated thrust [kN]	Absorbed power [kW]	Thrust/ power ratio [kN/kW]
PU	Universal, overhung	Pontoon type	64.88	868.5	0.0747
PP	Pontoon type	Pontoon type	68.03	881.4	0.0772
VP	Pontoon type	Traditional V(U)-shape	66.74	869.5	0.0768

PU hull shape—A combination of an overhung stern with a pontoon bow gave the worst performance values in the CFD analyses. This was due to the unfavourable flow around the simplified shape of the overhung stern. After reaching the stern overhang, the streamlines suddenly detached from the hull, creating intense vortices beneath the overhang and turbulence behind the ship's stern. This hull was designed as a universal solution to ensure comparability between the results for a distributed propulsion system and traditional stern arrangements; it is not considered a suiTable solution for real vessels.

PP hull shape—This hull, with a pontoon-shaped bow and stern, achieved the best performance parameters when operating with the distributed propulsion system shown in Fig. 2(c). Placing the propellers to the side of the hull allows for free shaping of the stern section, regardless of requirements such as the placement of the propeller in the tunnel, water supply, and tunnel shielding. In general, the pontoon termination gives a smoother transition to the cylindrical part of the hull, generates low bow waves at the ship's side, and creates more accepTable turbulence in the stern section. These favourable hydrodynamic properties were reflected in the simulation results.

VP hull shape—For historical reasons, we considered the V- or U-shaped stern, which is widely used on inland cargo ships. A combination of this with a pontoon stern achieved average performance in the CFD analyses. This bow shape generates relatively high waves in the transition area from the bow to the middle part of the hull, whose length, height parameters, and position depend on the navigation speed (at a constant water depth). For distributed propulsion systems, an unsTable water surface is very unfavourable, so the usability of a V- and U-shaped stern is very limited. It may have some justification on ships with a narrower hull, due to the milder bow waves, but as the T/B ratio increases it becomes less useful.

Although this study investigated propulsion performance at three relevant navigation speeds (3.0, 3.5, and 4.0 m/s), broader operational profiles that include variations in water level, channel cross-section, and sediment interaction are frequent in inland waterways. These factors can significantly affect the hydrodynamic resistance and propeller inflow conditions. Future simulations will focus on assessing the influence of variable water depths and unsteady flow regimes to generalise the applicability of the current findings.

DISCUSSION OF RESULTS

If overall thrust is the main selection criterion, Figure 9 can be extended into a design chart for choosing the most suiTable distributed-propulsion configuration. The current graph contains only the thrust curves for the arrangement shown in Fig. 2(c), a four-stage serial propulsion system. When the thrust curves of the three-stage and two-stage versions (as shown in Figs. 2(a) and (b)) are added, the graph can aid a ship designer in specifying the propulsion system for a specific designed vessel. Fig. 19 shows this design graph with the assumed thrust curves for all arrangements shown in Fig. 2.

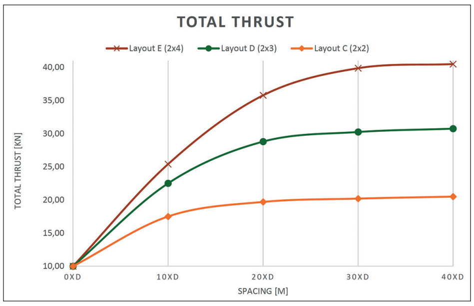

Fig. 19. Designer's graph showing total thrust for different layouts of identical propulsors

This expanded graph not only visualises the total thrust for the individual configurations but also serves as a preliminary design tool for optimising propulsion layouts during the early stages of ship design. This can significantly reduce time spent on iterative simulations, allowing for faster decision making in regard to hull-propulsor matching.

From Figs. 14–18, it is evident that at a given RPM, the propulsor with duct 7 achieves higher thrust and navigation speed than the propulsor with duct 8. Duct 8 has a certain power reserve compared to duct 7, which can be used to increase the thrust. When the geometric dimensions of the propulsion unit are maintained, this effect can be achieved by increasing the propeller's RPM. This observation highlights an important trade-off: whereas duct 7 is more efficient at standard RPMs, duct 8 provides more operational flexibility under varying power demand and sailing conditions.

In Fig. 18, at the equilibrium point of duct 8 and a navigation speed of 3.54 m/s, the difference in absorbed power is 14.28 kW. The correction value for the generated thrust can be obtained simply as the product of this difference and the thrust-to-power ratio at the equilibrium point. When this correction of 0.95 kN is added to the thrust at the equilibrium point, the maximum achievable thrust for duct 8 is 56.87 kN. This value can be compared with the maximum thrust of duct 7 at a navigation speed of 3.54 m/s (62.18 kN), which yields a difference in thrust of 9.3% in favour of duct 7, with the same absorbed power.

This calculation confirms that although duct 7 exhibits better performance, duct 8 remains a viable alternative if compensatory adjustments (e.g. an increase in RPM or changes to the blade pitch) are made.

Based on these considerations, it can be stated that both solutions for the propulsor are applicable in the given working range, with the proviso that to achieve comparable thrust and propulsor performance, duct 8 must operate at a higher RPM (or must have a greater pitch). Propulsors equipped with a throttling cone exhibit more sTable flow fields over time, which is likely to be due to reduced resonance and smoother pressure gradients. Furthermore, the propellers of these propulsion units are less loaded, since they are relieved by the additional thrust force generated on the cone surfaces on the discharge side of the duct. This contributes to improved mechanical longevity and potentially lower maintenance requirements over long-term operation, a key consideration for inland cargo vessels operating under variable draft conditions.

An additional reference analysis was conducted with the same hull equipped with a traditional stern arrangement of four (2+2) propulsors. This version initially yielded high performance in CFD analyses, generating thrust at the level of duct 7 with only 57% of the absorbed power. However, after a certain period, an insufficient water supply from the lower area of the ship (including the effect of suction) became apparent, and the intense flow gradually shifted to the side of the ship near the propulsors. This process was accompanied by a noticeable loss of propulsion power, and was terminated by the ventilation of the lateral propellers.

These transient effects reflect real-world limitations of traditional stern-mounted systems in shallow or restricted waters, and validate the shift toward distributed side-mounted configurations.

This outcome was as expected, and clearly supports the rationale for investigating distributed propulsion systems. Fig. 20 shows a bar graph with values of the generated thrust, absorbed power, and the ratio between them for the different configurations.

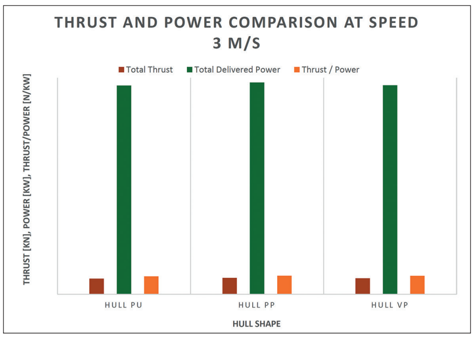

Fig. 20. Comparison of results for the thrust and power for propulsors interacting with different hull shapes

These simulations show that side-arranged distributed propulsion systems are most suited to hull terminations of the pontoon type, with a smooth transition to the cylindrical part. The pontoon-shaped ends effectively minimise flow separation and turbulence, especially in the stern region, thereby enhancing overall propulsion efficiency. Further investigation is needed to assess the impact of this system on boundary layer development, flow separation, and vortex formation. This finding highlights the need for high-fidelity turbulence models and possibly experimental validation through model tests or particle image velocimetry to improve the current understanding of flow-structure interaction. Based on the projected length of the vessel and the required total thrust, optimal parameters for the propulsion system, such as the propeller diameter, arrangement, and spacing between propulsion units, can easily be determined using performance curves. These curves should be compiled into a digital tool or software module to allow designers to input vessel dimensions and operational constraints, and to receive optimised propulsion layouts as outputs. There is a need to create these tools for all typical diameters for a specific type of propeller.

The first stage of the distributed propulsion study involved the development of a simplified hydrodynamic (CFD) model to explore potential propulsion arrangements. This narrowed the selection of models for the later stages of analysis, which included performance comparisons of various potential arrangements with a conventional twin-screw aft arrangement. Key conclusions were drawn about potential adverse operating scenarios under restricted-navigation conditions.

The second stage focused on examining and analysing the performance characteristics of the individual propulsion units, with the aim of finding a fundamental design for the most suiTable propeller/duct-type propulsion unit for operation within a distributed configuration under restricted navigational conditions. The outcomes included performance graphs for the individual propulsors, a comparison between them, and a conceptual 3D model of the most suiTable solution, which could be used as input for subsequent pre-production optimisation processes.

The third stage, as summarised in the study's results, involved investigating and analysing combinations of propulsion unit arrays and the ship's hull. We conducted performance analyses of the most advantageous distributed system arrangements near the vertical side of the hull at limited drafts. The result was a conceptual design chart of distributed propulsor arrays, which would allow a designer to determine the optimal number and distribution of units for a given set of dimensions for the main hull and for certain propulsors.

The aim of future research should be to integrate these stages into a unified parametric design platform, thus enabling iterative adjustments to be made in real time as new hull or propulsion configurations are introduced. In practice, a chart would be required for each specific propeller/duct type and size.

The CFD mesh included near-wall prism layers, which were used to resolve the boundary layer on the hull surface, particularly in the stern zone. The k–ω SST turbulence model used here enabled us to capture the separation and vortical structures relevant to shallow-draft flow regimes. Although not visualised here, this treatment ensured that the effect of the boundary layer was included in the resistance and thrust estimates.

CONCLUSION

This study has presented a novel methodological approach to investigating distributed propulsion systems under restricted navigation conditions. The primary theoretical contribution of this work lies in the relationships that were derived between the total system thrust and the propulsor spacing across different configurations. These graphs offer practical value in terms of the ship's design processes when tailored to specific propulsion units. The numerical implementation was carefully constructed using the k–ω SST turbulence model and mesh strategies to ensure appropriate near-wall resolution ($y^+ < 30$), and was validated against established CFD practices. Although experimental validation is left for future work, the numerical approach described here builds on previously verified duct geometries and validated CFD practices. Equipped with these tools, ship designers can develop initial conceptual designs for ships with distributed propulsion systems. A numerical self-propulsion evaluation confirmed that duct 8 achieved a slightly higher equilibrium speed than duct 7, with improved hydrodynamic coupling between the hull and distributed propulsors. This result offers quantitative support for the observed improvements in the efficiency of the duct 8 configuration, and provides a practical reference for optimising future designs of distributed propulsion systems.

This study of the impacts of distributed systems allows for the design of a next-generation ship at the conceptual stage. The primary characteristics of future shallow-draft inland vessels will include the following:

- Distributed propulsion system: The best results of the three shapes examined here for the ends of the vessel were achieved for a pontoon-shaped bow and stern. Long vessels (over 100 m) should be equipped with a distributed arrangement (E 4+4), with a pontoon-shaped bow and stern. Propulsion units must be retracTable or foldable from the side of the hull, and the side of the hull must be shaped so that the propellers can operate even when retracted, albeit with reduced power. Losses associated with the spacing of serially arranged propulsors are caused by the mutual influence of their flow fields; when the propulsor spacing is small, the accelerated water flow on the downstream side of the forward propulsor does not lose kinetic energy, thereby increasing the flow speed on the upstream side of the rear propulsor. As a result, the thrust force of the rear propulsor decreases as its efficiency increases. For the same reason, propulsors with high flow velocities on the downstream side must have larger spacings, and are generally not the most suiTable for this type of distributed system. From a technical perspective, a distributed system achieves the maximum possible performance with a spacing interval of 30D to 40D, where losses are negligible.
- Atypical (even extreme) aspect ratios of the main dimensions: This holds particularly true for very wide hulls of up to 24 m, with a large breadth-to-draft ratio and a small length-to-breadth ratio (where 24 m is the maximum possible vessel width in the Danube's locks from the Black Sea to Mohan). The appearance of such vessels will be significantly different from traditional ships with similar purposes, especially when combined with autonomous systems.
- Electrically powered propulsion units: These are the only feasible solution for driving the distributed propulsion system's units. The joint operation of numerous energy sources and propulsion units must be managed by an intelligent management system.
- Modular hull construction and functional units: As far as possible, the main functional units (e.g. propulsion units) should be designed in a modular manner to enable simple and quick exchange from the shore. This approach has the advantage that the repair and maintenance of functional units can be performed in a workshop during regular operation of the vessel. This feature becomes more relevant in the context of unmanned navigation.

Future work will focus on experimental verification and on extending the numerical framework to variable water depths and unsteady flow regimes.

ACKNOWLEDGEMENTS

This paper is the result of Project VEGA No.1/0312/25: Research on the economic efficiency of inland water transport, 2025-2027.

REFERENCES

1. Kendra M, Skrúcaný T, Dolinayová A, Čamaj J, Jurkovič M, Csonka B, Abramovic B. Environmental burden of different transport modes—Real case study in Slovakia. Transp Res Part D: Transp Environ2023, 114, 103552. doi: https://doi.org/10.1016/j.trd.2022.103552

2. Mako P, Galierikova A. Inland navigation on the Danube and the Rhine waterways. In 14th Int. Sci. Conf. on Sustainable, Modern and Safe Transport, TRANSCOM 2021. Slovakia, 26–28 May 2021.

3. Hasan SMR, Karim MM. Energy-efficient inland cargo ship design based on fuel consumption and CO_2 emission control using CFD. In Proc. 13th Int. Conf. on Marine Technology (MARTEC 2022), 4 Apr 2022. doi: http://dx.doi.org/10.2139/ssrn.4409979

4. Buchler D, Luck R, Markert M. Propulsion and control system for shallow water ships based on surface cutting double propellers. In Proc. 8th IFAC Conf.Control Appl. Mar. Syst.; Rostock-Warnemunde, Germany, 15–17 Sep 2010.

5. Zentari L, Moctar O, Lassen J, Hallmann R, Schellin TE. Experimental and numerical investigation of shallow water effects on resistance and propulsion of coupled pusher-barge convoys. Appl Ocean Res 2022,121,103048. doi: https://doi.org/10.1016/j.apor.2022.103048

6. Melnyk O, Onyshchenko S, Koryakin K. Nature and origin of

major security concerns and potential threats to the shipping industry. Sci J Silesian Univ Technol, Ser Transp 2021,113,145–153. doi: https://doi.org/10.20858/SJSUTST.2021.113.11

7. Melnyk O, Bychkovsky Y, Onishchenko O, Onyshchenko S, Volianska Y. Development of the method of shipboard operations risk assessment quality evaluation based on experts review. Stud Syst Decis Control 2023,481, 695–710. Springer. doi: https://doi.org/10.1007/978-3-031-35088-7_40

8. Vimala V, Veeramanikandan K, Viswanathan N, Pitchia Krishnan B, Hari S, Madhavan S, Dhinesh S, Karthikeyan V. Analysis of marine propeller using computational fluid dynamics. Mater. Today Proc. 2022,68(6),2375–2381. doi: https://doi.org/10.1016/j.matpr.2022.09.105

9. Wang D, Wang Y, Liu J, Hu Z, Zhang W, Wang Z, Jiang Y. An integrated dynamic modeling method for underwater vehicle with hull, propeller and rudder. Ocean Eng 2023,282,115036. doi: https://doi.org/10.1016/j.oceaneng.2023.115036

10. Aram S, Mucha P. Computational fluid dynamics analysis of different propeller models for a ship maneuvering in calm water. Ocean Eng 2023,276,114226. doi: https://doi.org/10.1016/j.oceaneng.2023.114226

11. Hekkenberg RG. Inland ships for efficient transport chains. PhD thesis, Delft University of Technology, 2013. doi: 10.4233/uuid:f2ead20f-80b5-4d92-818f-7586c7b85f76

12. Lackenby H. The effect of shallow water on ship speed. Shipbuilder Mar Eng 1963,70,446–450.

13. Raven H. A new correction procedure for shallow-water effects in ship speed trials. In Proc. 13th Int. Symp.Practical Design of Ships and Other Floating Structures (PRADS 2016), Copenhagen, Denmark, 4–8 Sep2016.

14. Schlichting O. Schi_widerstand auf beschränkter wassertiefe: Widerstand von seeschi_en auf flachemwasser [Ship resistance in restricted water depth: Resistance of sea-going vessels in shallow water]. Jahrb Schi_bautech Ges 1934, 35,127.

15. Ferreiro LD. The effects of confined water operations on ship performance: A guide for the perplexed. Nav Eng J 1992,104, 69–83.

16. Rotteveel E, Hekkenberg R, Ploeg A. Inland ship stern optimization in shallow water. Ocean Eng 2017,141,555–569.

17. Tuck EO. Hydrodynamic problems of ships in restricted waters. Annu Rev Fluid Mech 1978, 10,33–46.

18. Saha GK, Suzuki K, Kai H. Hydrodynamic optimization of ship hull forms in shallow water. J Mar Sci Technol 2004,9, 51–62. doi: 10.1007/s00773-003-0173-3

19. Franceshi A, Piaggio B, Villa D, Viviani M. Development and assessment of CFD methods to calculate propeller and hull impact on the rudder inflow for a twin-screw ship. Appl Ocean Res 2022,125,103227. doi: https://doi.org/10.1016/j.apor.2022.103227

20. Melnyk O, Onishchenko O, Onyshchenko S, Shumylo O, Volyanskyy S, Bondar A, Cheredarchuk N. Application of fuzzy controllers in automatic ship motion control systems. Int J Electr Comput Eng 2023,13,4,3948–3957. doi: https://doi.org/10.11591/ijece.v13i4.pp3948-3957

21. Shumylo O, Yarovenko V, Malaksiano M, Melnyk O. Comprehensive assessment of hull geometry influence of a modernized ship on maneuvering performance and propulsion system parameters. Pomorstvo 2023,37,2,314–325. doi: https://doi.org/10.31217/p.37.2.13

22. Ferziger JH, Peric M. Computational methods for fluid dynamics. Springer, Berlin Heidelberg, 2002. doi: 10.1007/978-3-642-56026-2

23. Illes L, Jurkovič M, Kalina T, Gorzelanczyk P, Ľupták V. Methodology for optimising the hull shape of a vessel with restricted draft. Sci J Silesian Univ Technol Ser Transp 2021,110,57–71. ISSN: 0209-3324. doi: 10.20858/sjsutst.2021.110.5

24. Illes L, Kalina T, Jurkovic M, Luptak V. Distributed propulsion systems for shallow draft vessels. J Mar Sci Eng 2020, 8,667. doi: https://doi.org/10.3390/jmse8090667

25. Illes L, Jurkovic M, Kalina T, Sosedova J, Gorzelanczyk P, Stopka O, Kubjatko T. Concept and performance analysis of propulsion units intended for distributed ship systems. J Mar Sci Eng 2022, 10,448. doi: https://doi.org/10.3390/jmse10040448

26. Kudelas D. Basic of computer flow modelling and visualization. Faculty of Mining, Ecology, Process Control and Geotechnologies: Kosice, Slovakia, 2017.